International Journal of Engineering Trends and Technology
ISSN: 2231 – 5381 / https://doi.org/10.14445/22315381/IJETT-V70I5P205

Volume 70 Issue 5, 30-36, May 2022

Original Article

Experimental and Finite Element Analysis of Carbon Fibre Fabric/Polypropylene Composites under Different Processing Parameters

Subrata Debnath[1], Joyshri Rava[2], Arun Jyoti Dev Sharma[3], Sushen Kirtania[4], Satadru Kashyap[5], and Sanjib Banerjee[6]

[1,2,3,4,5,6] *Department of Mechanical Engineering, Tezpur University, Tezpur-784028, Assam, India.*

sushen@tezu.ernet.in

Received: 19 January 2022 Revised: 04 April 2022 Accepted: 26 April 2022 Published: 19 May 2022

Abstract *- Carbon fiber fabric (CFF)/maleic anhydride coated isotactic polypropylene (PP) composites were fabricated under different compression molding temperatures and pressures to study the effect of these processing parameters on the tensile properties of the composites. Preliminary tensile testing revealed that CFF in the plain-weaved (PW) form exhibited superior tensile properties than longitudinal (parallel) strands of CFF. Subsequently, PW CFF was used as a reinforcing agent in the PP matrix, and composites were fabricated under varying levels of compression pressure (100 kg/cm2, 80 kg/cm2, and 60 kg/cm^2) and temperature (180 °C, 160 °C, and 157 °C). It was observed that compression pressure and temperature were instrumental in deciding the tensile properties of the composites. The compression pressure of 60 kg/cm2 and temperature of 157 °C yielded the composite with the highest tensile strength and flexibility.*

Additionally, surface-modified CFF reinforced PP composite exhibited maximum strength among all the composites studied. Finite element (FE) analysis has also been done to compare the experimental results. Experimental values of Young's moduli were revealed to be higher than the simulated results, as the FE model was based on certain assumptions. However, both the stress-strain curves are comparable within the elastic limit.

Keywords *- Carbon fiber fabric, Polypropylene, Tensile strength, Processing parameters, Finite element analysis.*

1. Introduction

In recent times, carbon fiber (CF) reinforced composites have been used in different areas ranging from construction and sports to aeronautics [1] and automotive sectors [2,3], among others. The primary reason behind such applicability of polymer composite materials reinforced with CF is that they exhibit mechanical properties equivalent to conventional metallic materials and have the major advantage of higher strength to weight ratio and stiffness to weight ratio [2, 4]. Among the polymeric matrices, polypropylene (PP) is largely used in engineering applications as it is thermo-formable and has comparable mechanical properties with contemporary polymers. The difference between the melting temperatures of carbon fiber fabric (CFF) and PP has been utilized to fabricate all CFF/PP composites. The latter must be liquid for effective adhesion of reinforcement and matrix, ensuring good wetting and penetration between the fiber fabrics. Still, severely high temperatures must be avoided that can cause melting and degradation of the fiber fabric [5,6,7]. Despite the numerous advantages of fiber-reinforced composites over their metallic counterparts, the former is more vulnerable to mechanical damage when exposed to high tension, compression, or impact leading to failure [8-10]. Hence, a detailed investigation of their mechanical properties is of prime importance.

A compressive review on fabric reinforced laminated composites has been presented by Hasan et al. [11] and reported their performances. Paiva et al. [12] investigated the mechanical properties of various CF, and epoxy resin composites consisting of combinations of plain weaved (PW). Eight harness satin (8HS) CF weaving patterns and two epoxy matrices, following ASTM D3039 standards with the reinforcement to matrix ratio of 60:40. The strength of the weaving pattern was also compared when PW displayed the higher yield strength, but on the contrary, 8HS yielded the higher elastic modulus. Szpieg et al. [13] fabricated a fully recycled CF (rCF) and modified polypropylene (rPP) composite. The volume fraction of the fiber was kept at 40% of the entire composite specimen volume. Four different types of specimens were prepared according to the direction of rCF, *i.e.*, 0˚, 45˚, and ±90˚, to evaluate the variations in tensile strength. Zhang et al. [14] performed oxidation on CF by heating them in nitric acid (65–68 wt%) at 90 °C for 1.5 h and reported the improvement of the bonding strength between the fibers and the matrix. Tiwari et al. [15] used boiling nitric acid (65-68 wt%) at 110 °C for oxidizing CFs for a total duration varying from 15 to 180 min. The increases in chemical reactivity of the fibers and the resulting wettability with the matrix were steep up to 60 min, while more gradual and slower until 90 min. It was also reported that tensile strength decreased with an increase in treatment time, and the load-bearing capacity of the fibers decreased by 40% after 3 h. Ravandi et al. [16] reported the mechanical behavior of knitted CFF reinforced composite under tensile loading. They have also compared their experimental results with FE simulation results and reported a good agreement between these two results. Elanchezhian et al. [17] fabricated and investigated the mechanical behavior of CF reinforced polymer composite (CFRPC) and glass fiber (GF) reinforced polymer composite (GFRPC) under different types of loading conditions. They have also reported that the CFRPC shows better properties than the GFRPC under tensile and flexural loading. Experimental investigation and finite element analysis (FEA) have been performed to investigate the behavior of square hollow steel sections bonded with CFRP fabric [18]. Subramonian et al. [19] fabricated alkali-treated bagasse fiber PP composites and investigated the weight percentage of bagasse fiber on tensile, flexure, and hardness characteristics. The maximum and minimum tensile strengths were reported for 30 wt% and 10 wt% of fiber. Experimental investigation and FEA have been performed on fiber-reinforced polymer composite (FRPC) strut considering different laminated stacking sequences and reported that strut with 30^o orientation of fiber angle exhibit better results [20]. Tavashi et al. [21] reported that the strength of steel structure could be increased by bounding different types of FRP sheets.

Although a considerable amount of research is prevalent on CF reinforced composites, detailed investigations on CFF reinforced polypropylene composites are still limited. The present study involves an experimental evaluation of the tensile properties of compression-molded CFF/PP composites as a function of the processing parameters (temperature and compression pressure). Additionally, the effects of surface treating the CFF with nitric acid (HNO_3) on the tensile properties were also investigated. The CFF/PP specimen simulation was also done using commercial software ANSYS to evaluate the elastic modulus. The computational results were successfully compared and correlated with the experimental values.

2. Materials and Methods

2.1. Materials

For the fabrication of the composite specimens, CFF (12K UD Fabric 200 gsm, Supplier: Jalark Carbon Products) of diameter 12 mm was used as the reinforcing material. Maleic anhydride grafted isotactic PP (Maker: Aldrich, Product code: 428116) was used as the matrix material. Maleic anhydride enhances the surface properties of PP, which improves the interfacial bonding between the fiber and the matrix. The data provided by the supplier was further correlated with the published literature [22] to determine the mechanical properties of the presently used CFF material. The mechanical properties of CFF are listed in Table 1.

Table 1. Mechanical properties of CFF

Elastic Modulus [GPa]			Shear modulus [GPa]			Poisson's ratio		
E_x	E_y	E_z	G_{xy}	G_{yz}	G_{xz}	ν_{xy}	ν_{yz}	ν_{xz}
232	13	13	4.45	13.31	13.31	0.46	0.0168	0.0168

The elastic modulus and Poisson's PP ratio are 1.3 GPa and 0.42, respectively.

2.2. Fabrication Procedure

To facilitate the adhesion of CFF and PP during the molding process, a mild steel (MS) mold was fabricated. The design of the mold included both cope and drag with MS strips which could be easily screwed tight with the base plate. This allowed for easy clamping of the CFF strips before the compression process and easy removal of the final product. for the molding process, a semi-automatic compression molding machine (MAKE: SANTEC, Model: SCM-15) was employed, with a pressing capacity of 15 tons, plate area of 200 × 200 mm^2, and a peak heating temperature of 250 ˚C. in such a molding machine, the mold stays in constant contact with the press plates while heat and pressure are continuously maintained until the complete cure of the molding material.

Initially, to understand the effect of fiber orientation on the composite properties, two types of samples were tested: (a) one where all the fibers were longitudinally placed parallel to each other, *i.e.*, no weave (NW), and (b) one where the fibers were plain weaved (PW). for the present investigation, PW orientation of fiber was chosen since being the tightest weave, it is least prone to fray at the ends, and the easiest to work with [12]. During manual plain weaving, at first, strands of CFF were segregated from the mat form and were wrapped on a ring of 25 mm width. Another strand of CFF was knotted in a needle made of steel wire. This strand was then weft in the wrapped present on a 1 × 1 weave design wire. The same weaving pattern was continued for a length of 250 mm. for matrix material, PP and maleic anhydride granules were manually crushed into fine particles and subsequently mixed thoroughly for 1.5 h in a blender.

For fabrication of the CFF/PP composites, a layer (5 mm thick) of mixed PP and maleic anhydride powder was kept on the base plate, the PW CFF followed this, and finally, another layer (5 mm thick) of mixed PP and maleic anhydride powder were distributed uniformly on the top. During the current study, the composites were investigated for a fiber-matrix volumetric ratio of 60:40 [12]. Fig. 1 (a) and Fig. 1 (b) show the PW CFF and powder PP in the mild steel mold, respectively.

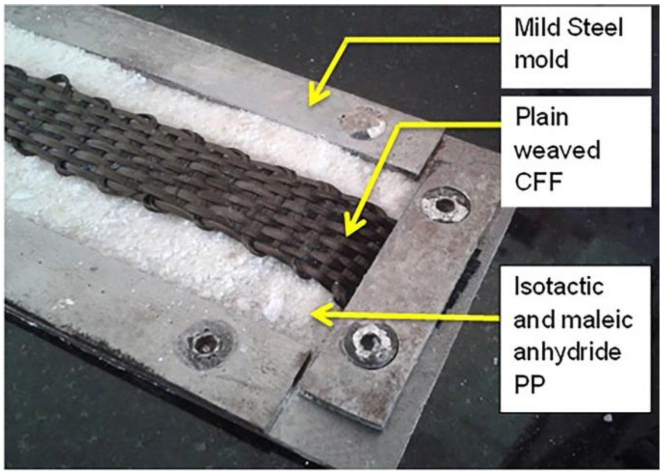

(a)

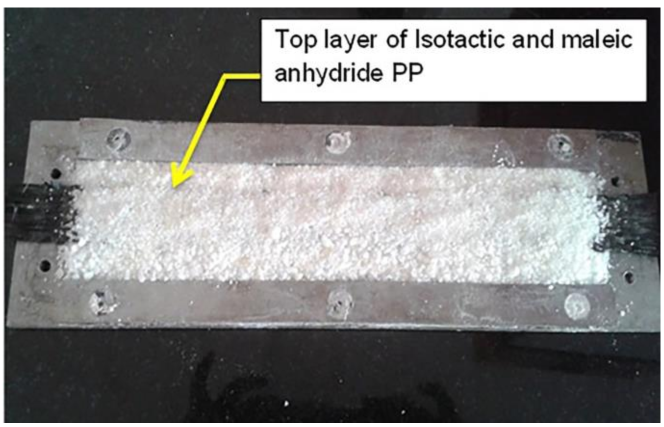

(b)

Fig. 1 (a) Plain-weaved CFF and (b) powder PP in the mold

2.3. CFF/PP composite

The main objective of this present work is to study the mechanical properties of the CFF/PP composites as a function of processing parameters such as temperature and compression pressure during molding. Hence, the fabricated composites were categorized based on the peak temperature and pressure during compression molding, which varied to evaluate the optimal parameters required to exhibit the best mechanical properties. During compression, all the samples were kept under constant heat and pressure for 5 min and subsequently cooled for 2 h inside the compression plates [12, 19]. The molding temperature varied at 180 °C, 163 °C, and 157 °C, while the pressure was respectively varied as 100 kg/cm^2, 80 kg/cm^2, and 60 kg/cm^2. The various processing parameters employed during the compression molding and the corresponding categories of the samples are listed in Table 2.

Table 2. Variation in processing parameters during compression molding of CFF/PP composites

Specimen designation	Temperature (°C)	Pressure (kg/cm^2)
180/100	180	100
163/80	163	80
157/60	157	60
157/60(E)	157	60

2.4. Surface treatment of CFF

It has been reported from earlier studies that surface properties of fibers are affected by surface treatment via etching processes, which alters the stiffness of the carbon strands and enhances the interfacial bonding between the fibers and matrix in a composite [14, 15]. Thereby the weaved fibers were immersed in 60% aqueous nitric acid solution at 120 ˚C refluxing temperature for 2 h in a hot air oven (MAKE: GENAXY, Model: RN series) [14, 15]. After the fibers were cooled down to room temperature, they were subsequently properly washed under running cold water to remove all traces of the acid. These fibers were then used to fabricate surface-treated CFF/PP composites designated as 157/60(E) (refer to Table 2), and their mechanical properties were evaluated.

The CFF/PP composite specimens were fabricated as per ASTM D3039 standard. The dimensions of the samples were 250 mm × 25 mm × 4 mm. It is commonly observed that the grips of a tensile testing machine impose significant stress concentration on the specimen. To minimize this effect, 220 Grade SiC paper was used for the gripping purpose of every sample (Fig. 2) [12].

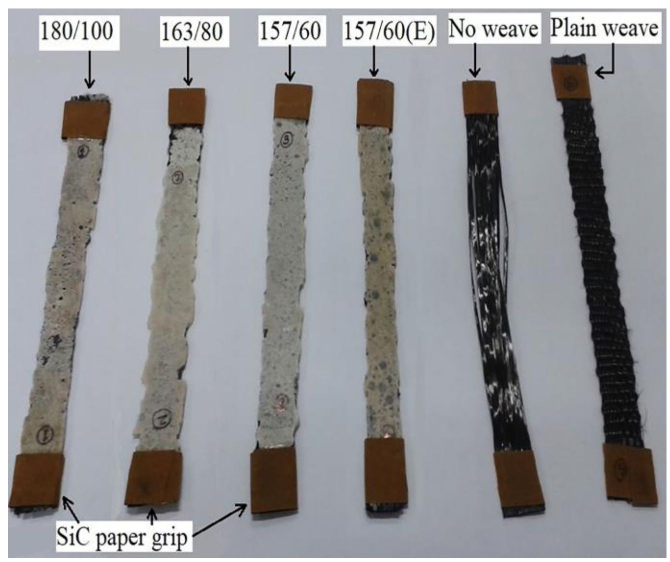

Fig. 2 CFF/PP composite and CFF specimens

2.5. Tensile Testing

The mechanical properties were evaluated in terms of the tensile properties of the composites. The uniaxial tensile test was conducted using a 100 KN dynamic testing machine

(INSTRON, 8801). As depicted in Fig. 2, all the specimens were tensile tested with a given strain rate of 1 mm/min as per ASTM D3039 standard. The mountings of the CFF/PP specimen and PW CFF specimen before the testing are displayed in Fig. 3 (a) and Fig. 3 (b), respectively.

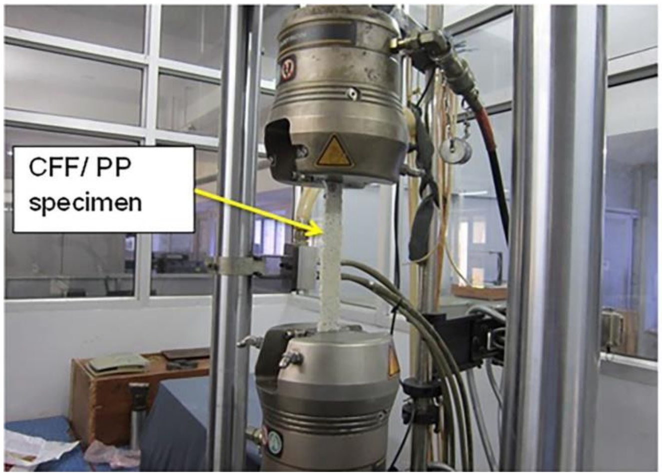

(a)

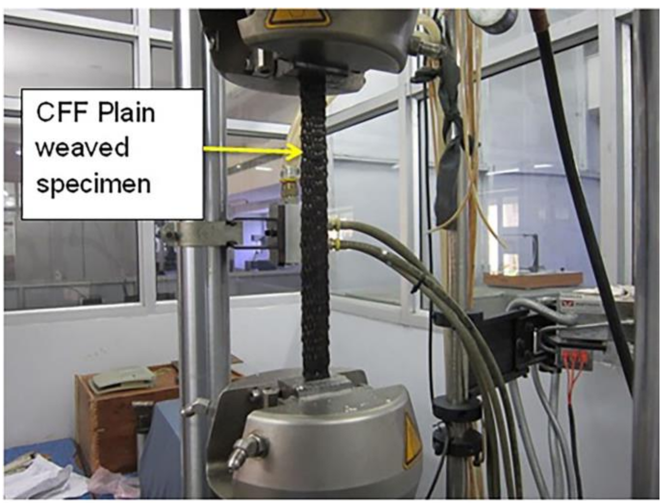

(b)

Fig. 3 Mounting of (a) CFF/PP (b) Plain weaved CFF specimens during tensile testing

2.6 Finite Element Modeling

For the FE analysis, CFF/PP composite, CFF, and PP specimen models have been simulated using ANSYS. The element used for the FE simulation is SOLID45. The dimension of the model was according to the ASTM D3039 standard *i.e.*, length (l) = 0.250 m (in z-direction), width (w) = 0.025 m (in x-direction) and thickness (t) = 0.004 m (in y-direction). The FE model, along with three CFF/PP composites layers, is shown in Fig. 4. The number of nodes and elements of the FE model are 215271 and 200000, respectively. The boundary condition is: degree of freedom is zero for all nodes at z = 0. But a variable force has been applied to all the nodes at z = 250 mm, *i.e.*, at the end surface of the model.

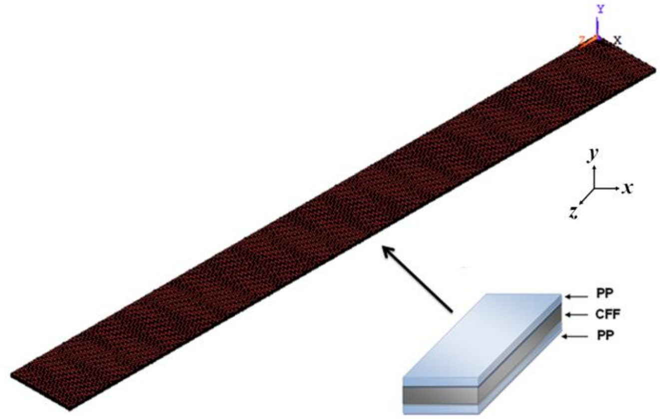

Fig. 4 The FE model, along with three layers of CFF/PP composite

The FE mesh of the composites is also shown in Fig. 5 by considering one-fourth of the actual length and half of the actual thickness and width of the composite sample to understand the FE mesh clearly.

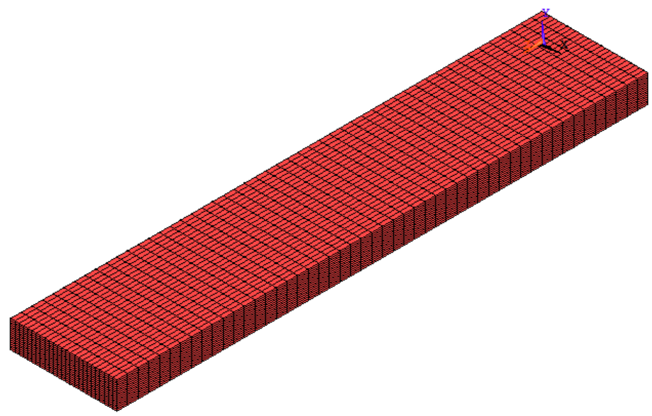

Fig. 5 The FE mesh of the CFF/PP composite

3. Results and Discussion

CFF/PP composites were presently fabricated under varying compression molding temperatures and pressure to investigate the effects of these processing parameters on the tensile properties of the composites. A comparative analysis was also conducted between the experimental values and values obtained from the FE simulation to further validate the predicted model.

3.1 Comparison of Carbon Fiber Fabric Strength

Initially, to investigate fiber orientation's effect on the composites' mechanical characteristics, tensile properties of the NW (longitudinal parallel strands) and PW CFF samples were estimated. Fig. 6 shows the experimentally obtained engineering stress vs. strain plots for NW and PW CFF specimens.

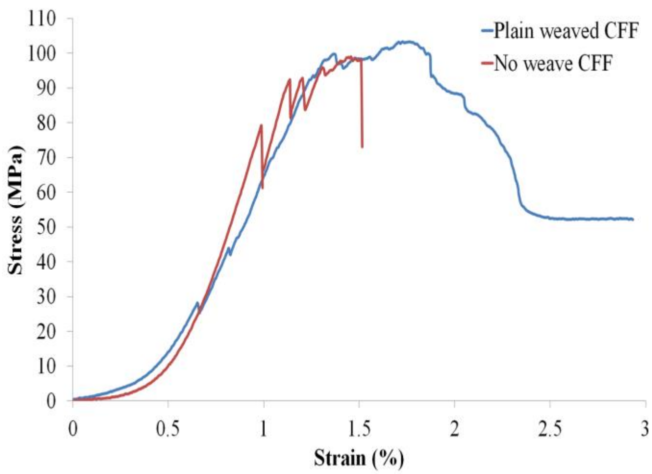

Fig. 6 Experimentally obtained engineering stress-strain plots for NW and PW CFF specimens

The tensile strength of the PW CFF specimen (103.28 MPa) is 4.38% more than that of the NW specimen (98.95 MPa), but Young's modulus for the PW CFF specimen (11.32 GPa) is less by 27.39% as compared to NW CFF specimen (14.42 GPa) [12]. Similar types of stress-strain plots of CFRPC and GFRPC under tensile loading have been reported by Elanchezhian et al. [17]. The superior tensile strength indicated that the PW of the strands has resulted in higher strength of the specimen due to its fiber arrangement. Plain weave leads to a better distribution of the acting load, generating a higher strength level. PW samples also provided better ductility by exhibiting higher elongation before failure due to better stress distribution upon loading. Therefore, in the current investigation, PW CFF was used to fabric CFF/PP composites.

3.2 Analysis of CFF/ PP composite

3.2.1 Experimental Investigation

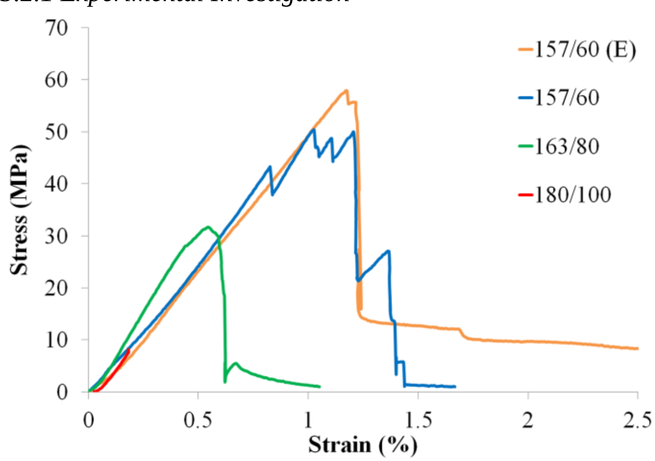

Fig. 7 Experimentally obtained engineering stress-strain plots of all the composite samples

All the CFF/PP composites were subjected to uniaxial tensile testing to study their properties under uniaxial stress in the longitudinal direction. A lower strain rate of 1 mm/min was used per ASTM standards. Fig. 7 shows the stress vs. strain plots for CFF/PP composites of 180/100, 163/80, 157/60, and 157/60(E) specimens. Table 3 lists the tensile properties of all the samples.

Table 3. Tensile properties of all the composite samples

Specimen designation	Tensile strength (MPa)	Yield strength (MPa)	Young's modulus (GPa)	Elongation (%)
180/100	8.12	8.10	6.32	0.18
163/80	31.68	26.66	7.32	1.49
157/60	50.37	46.68	5.49	1.69
157/60(E)	57.88	51.83	5.46	2.54

It was observed from the tensile results that the mechanical strength (both tensile and yield) of the composites increased with a decrease in processing temperature and pressure. The specimen subjected to the highest temperature and pressure displayed the lowest yield strength, which may be attributed to the softening of the CFF. There is a radical improvement in the strength when the temperature and pressure are lowered. The specimen subjected to a temperature of 157 ˚C and pressure of 60 kg/cm^2 exhibited the highest strength among the investigated composites without any surface treatment, indicating the corresponding operating parameters best suited for fabrication of CFF/PP composites yielding the highest strength values. Better physical interaction and entanglement of the CFF fiber with hydrophobic PP chains led to higher tensile strength. However, it was also found that surface-treated CFF (etched with HNO_3) yielded the maximum strength among all of the composites considered. This revealed that surface modification of the CFF has led to high adhesion between the CFF and PP matrix at the fiber-matrix interface due to the generation of van-der-Waals forces and hydrogen bonding [14]. Elevated mechanical adhesion of the PP matrix provided by the rough surface-treated CF has resulted in better stress transfer at the fiber-matrix boundary, leading to high tensile and yield strength values.

However, it was observed that the elastic modulus increased when the compression temperature and pressure decreased from 180 °C and 100 kg/cm^2 to 163 °C and 80 kg/cm^2. This fact suggests that proper composite consolidation occurs at 157 °C and 60 kg/cm^2, which leads to higher rigidity within the elastic limit. The increase in the elastic modulus may be attributed to the replacement of the PP matrix with rigid CFF fibers and the restriction of the mobility of PP chains due to the addition of fibers, thus hindering deformation within the elastic limit. However, as the temperature and pressure are further lowered, the elastic modulus again decreases, leading to higher mobility of the PP chains upon stress application, thus lowering the rigidity within the elastic limit.

An increase in the elongation limit with decreasing temperature and pressure indicates that interfacial bonding between filler and matrix improved with decreasing processing parameters, thereby promoting better stress transfer between fiber and matrix. Further flexibility can be improved when the fibers are etched with HNO_3, which provides a rougher interface for the PP chains to adhere to. This provided higher interfacial adhesion at the CFF-PP interface, causing higher elongation before final failure.

3.2.2 Finite element analysis

The stress and strain values have been determined along the specimens' z-axis under different applied loads to compare and correlate with the experimental results. The maximum tensile stress and strain values have been estimated at $x = w/2$, $z = l$, and $y = 0$ to t, i.e., at the middle of the cross-section along the y-direction. This FE simulation result was used to determine Young's modulus of CFF/PP composites, and its value was evaluated to be 4.78 GPa.

3.3 Comparison of experimental and simulation results

Fig. 8 shows the stress vs. strain plots within the elastic limit considering experimental and FE results. Fig. 9 shows the magnified truncated view of the same stress-strain curves.

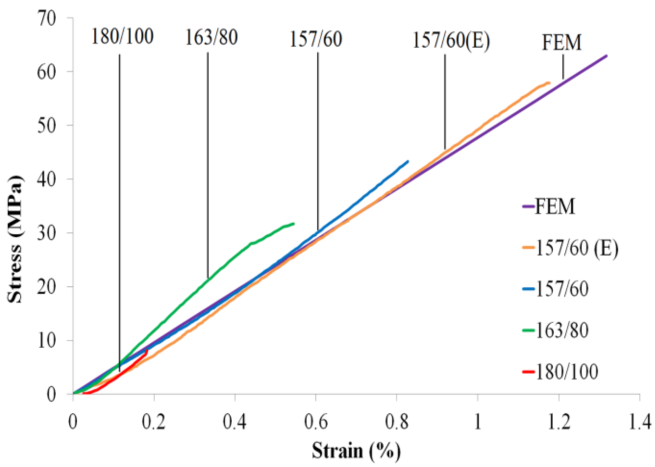

Fig. 8 Stress-strain curve showing the comparison between experimental and simulated Young's modulus values

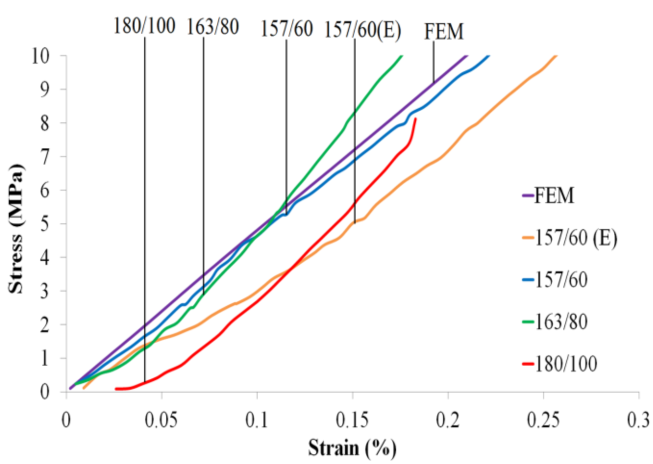

Fig. 9 Truncated stress-strain curve showing the comparison between experimental and simulated Young's modulus values

From the comparative analysis of the simulated and experimental values, Young's moduli of all the fabricated composites have been higher than the corresponding simulated values. Various reasons may be attributed to the superior properties of fabricated composites compared to the simulated results. The deviation between the experimental and the simulated data is due to the inability of the simulated model to account for the bonds that exist between the reinforcement and the matrix materials. Also, for the FE model, it was assumed that there is no differential elongation of fiber and matrix. Additionally, the weaving employed between the CFF strands is PW which is not accounted for in the simulated model. Hence, a difference is observed between the experimental and simulated results. However, Fig. 8 shows that the stress-strain curve obtained from the FE simulation is comparable with the experimental stress-strain curves within the elastic limit.

4. Conclusion

In the current research, the effects of processing parameters on the tensile properties of CFF/PP composites have been studied. Composites were fabricated under varying levels of compression pressure and temperature. The temperature was varied to 180 °C, 160 °C, and 157 °C, while compression pressure was varied in 100 kg/cm^2, 80 kg/cm^{2,} and 60 kg/cm^2. Additionally, in one sample, the CFF was surface treated with HNO_3 before being used as reinforcement in CFF/PP composites. The following important conclusions are listed from the current investigation:

- It was observed that PW CFF strands are stronger than NW CFF strands under tensile stress.
- Young's modulus for the PW CFF specimen is less by 27.39% than the NW CFF specimen.
- The optimum process parameters for 60% CFF reinforcement and 40% PP (isotactic and maleic anhydride) are 157 ˚C and 60 kg/cm^2. Specimens under such processing conditions exhibited the highest tensile and yield strength values.
- Tensile strength and flexibility of the CFF/PP composite improved upon treatment of the CFF with HNO_3 due to better adhesion at the fiber-matrix interface.
- The Young's moduli obtained experimentally are higher than the corresponding values obtained through FE simulation. The differences between the two results are due to certain assumptions considered during FE simulation, the primary one being the absence of PW in the CFF reinforcement.
- The stress-strain curves obtained from FE simulation and experiment are comparable within the elastic limit.

Author's Contribution Statement

SD, JR, and AJDS performed the fabrication of the composite specimens. SD and S Kirtania conducted the FEM analysis of the specimens. S Kirtania performed the tensile

tests of the specimens. SD, S Kirtania, S Kashyap, and SB wrote the manuscript. All authors read and approved the manuscript.

Conflict of Interest

The authors declare that they have no conflict of interest.

Funding

Financial support was received from Tezpur University to purchase consumables and process the materials.

Acknowledgment

The CFF/PP composite specimens were fabricated using compressing molding machine at the Department of Chemical Sciences, Tezpur University, and with the copious assistance from Mr. Nipu Dutta (Technical Assistant). Mr. Pranjol Paul (Technical Officer) and Sanjib Sarma (Senior Technical Superintendent) of Mechanical Engineering Dept., IIT Guwahati, have extended their help during the tensile testing of composites samples. Finite element simulations have been performed in the CAD laboratory at the Department of Mechanical Engineering, Tezpur University.

References

[1] Schwartz, MM (1997) Composite Materials Volume I: Properties, Nondestructive Testing, and Repair (1st Ed.). Prentice-Hall, United States , (1997).
[2] Buehler, F.U., and Seferis, J.C., Effect of Reinforcement and Solvent Content on Moisture Absorption in Epoxy Composite Materials, Composites Part A: Applied Science and Manufacturing. 31(7) (2000) 741-748.
[3] Hayes, B.S, Gilbert, E.N., and Seferis, J.C., Scaling Complications of Dual Temperature Cure Resin Prepreg Systems in Airplane Part Manufacture, Composites Part A: Applied Science and Manufacturing. 31(7) (2000) 717-725.
[4] Baker, AA, Callus, P.J., Georgiadis, S., Falzon, P.J., Dutton, S.E., and Leong, K.H., An Affordable Methodology for Replacing Metallic Aircraft Panels With Advanced Composites, Composites: Part A: Applied Science and Manufacturing. 33(5) (2002) 687-696.
[5] Houshyar, S., Shanks, R.A., and Hodzic, A., The Effect of Fiber Concentration on Mechanical and Thermal Properties of Fiber Reinforced Polypropylene Composites, Journal of Applied Polymer Science. 96 (2005) 2260–2272.
[6] Houshyar, S., Shanks, R.A., and Hodzic, A., Tensile Creep Behavior of Polypropylene Fiber Reinforced Polypropylene Composites, Polymer Testing. 24(1) (2005) 257–264.
[7] Houshyar, S., Shanks, R.A., and Hodzic, A., Influence of Different Woven Geometry in Poly(Propylene) Woven Composites, Macromolecular Materials, and Engineering. 290 (2005) 45–52.
[8] Moura, MFSF De, and Marques, A.T., Prediction of Low-Velocity Impact Damage in Carbon-Epoxy Laminates, Composites Part A: Applied Science and Manufacturing. 33(2) (2002) 361-368.
[9] Ding, Y.Q., Yan, Y., and Mcilhagger, R., Effect of Impact and Fatigue Loads on The Strength of Plain Weave Carbon-Epoxy Composites, Journal of Materials Processing Technology. 55 (1995) 58-62.
[10] Gao, S.L., and Kim, J.K., Cooling Rate Influences in Carbon Fiber/PEEK Composites, Part III: Impact Damage Performance, Composites Part A: Applied Science and Manufacturing. 32(6) (2001) 775-785.
[11] Hasan K.M.F., Horvath P.G., and Alpar T., Potential Fabric-Reinforced Composites: A Comprehensive Review, Journal of Materials Science. 56 (2021) 14381-14415.
[12] Paiva, J.M.F. De, Mayer, S., and Rezende, MC, Comparison of Tensile Strength of Different Carbon Fabric Reinforced Epoxy Composites, Materials Research. 9(1) (2006) 83-89.
[13] Szpieg, M., Wysocki, M., and Asp, L.E., Mechanical Performance and Modeling of A Fully Recycled Modified CF/PP Composite, Journal of Composite Materials. 46(12) (2011) 1503–1517.
[14] Zhang, X.R., Pei, X.Q., and Wang, Q.H., The Effect of Fiber Oxidation on The Friction and Wear Behaviors of Short-Cut Carbon Fiber/Polyimide Composites, Express Polymer Letters. 1(5) (2007) 318–325.
[15] Tiwari, S., Bijwe, J. and Panier, S., Tribological Studies on Polyetherimide Composites Based on Carbon Fabric With Optimized Oxidation Treatment, Wear. 271 (2011) 2252-2260.
[16] Ravandi M, Moradi A, Ahlquist S, and Banu M., Numerical Simulation of The Mechanical Behavior of A Weft-Knitted Carbon Fiber Composite Under Tensile Loading, Polymers. 14 (2022) 451.
[17] Elanchezhian C., Ramnath BV, and Hemalatha J., Mechanical Behavior of Glass and Carbon Fiber Reinforced Composites At Varying Strain Rates and Temperatures, Procedia Materials Science. 6 (2014) 1405-1418.
[18] Ranjith K., Ajeez A.A., Balagurunathan P., Structural Performance of Square Hollow Structural Steel (Shs) Tubular Section Under Axial Load Using Carbon Fiber Reinforced Polymer Fabrics, International Journal of Engineering Trends and Technology. 47(5) (2017) 295-302.
[19] Subramonian, S., Ali, A., Amran, A., Sivakumar, LD, Salleh, S., and Rajaizam, A., Effect of Fiber Loading on The Mechanical Properties of Bagasse Fiber–Reinforced Polypropylene Composites, Advances in Mechanical Engineering. 8(8) (2016) 1–5.
[20] Vijayasree K., Ravishankar D.V., and Reddy P.R., Critical Analysis of The Strut Made of Fiber-Reinforced Polymer Tested Under One End Hinged and The Other End Free, International Journal of Mechanical Engineering. 7(4) (2020) 29-33.
[21] Tavashi S., Kshirsagar V.S., Kapase R., and Thorat A., Flexural Behavior of Steel I–Beams Bounded With Different Fiber-Reinforced Polymer Sheets, International Journal of Engineering Trends and Technology. 54(2) (2017) 135-140.
[22] Herreaz, M., Mora, D., Naya, F., Lopes, C.L., Gonzalez, C., and Llorca, J., Transverse Cracking of Cross-Ply Laminates: A Computational Micromechanics Perspective, Composites Science and Technology. 110 (2015) 196-204.